Study of a millimeter-wave squint indirect holographic algorithm suitable for imaging with large field-of-view*

Gao Xiang(高 翔)[a)b)†], Li Chao(李 超)[a)b)‡], and Fang Guang-You(方广有)[a)b)]

[a)] Institute of Electronics, Chinese Academy of Sciences, Beijing 100190, China
[b)] Key Laboratory of Electromagnetic Radiation and Sensing Technology, Chinese Academy of Sciences, Beijing 100190, China

(Received 4 February 2013; revised manuscript received 19 March 2013; published online 10 December 2013)

In this paper a millimeter-wave (MMW) squint indirect holographic method is presented, which is suitable for imaging with a large field-of-view. The proposed system employs the squint operation mode to remove the background and twin-image interferences, which achieves a similar effect to off-axis holography but leaves out the large-aperture quasi-optical component. The translational scanning manner enables a large field of view and ensures the image uniformity, which is difficult to realize in off-axis holography. In addition, a corresponding imaging algorithm for the presented scheme is developed to reconstruct the image from the recorded hologram. Some imaging results on typical objects, obtained with electromagnetic simulation, demonstrate good performance of the imaging scheme and validate the effectiveness of the image reconstruction algorithm.

Keywords: millimeter-wave (MMW) indirect holographic scheme, squint operation mode, translational scanning manner, large field-of-view, image uniformity

PACS: 84.40.–x, 84.40.Xb **DOI:** 10.1088/1674-1056/23/2/028401

1. Introduction

Indirect holographic imaging technology, originally proposed by Gabor[1] who intended to improve the resolution of electron microscopes, has been rapidly developed and widely applied in optics.[2] The main characteristic of the indirect holography which gains the attention of so many researchers is its two step imaging process: hologram recording and image reconstruction. In the first step, two coherent waves interfere on an aperture, one is a target wave which is the scattered field from the target illuminated by a coherent source and the other is a reference wave which is a portion of the illumination wave and propagates directly to the aperture. The resulting interference pattern of the target and reference wave is then measured by a detector and recorded to form a hologram for imaging processing. The second step aims to retrieve the amplitude and phase of the target wave from the recorded hologram and reconstruct the image of the target with some numerical reconstruction algorithms. As only the modulus of field is measured, indirect holographic imagers often employ simple receiver technology, which greatly reduces the cost of system. Due to this advantage, indirect holographic technology has been used in millimeter-wave (MMW) imaging systems these years to leave out the expensive MMW heterodyne transceivers.[3–5] Compared with optics, MMW imaging has a lot of advantages which make a good compromise between spatial resolution and penetrating capability.[6–8]

Generally, MMW indirect holographic imaging can be divided into inline[9] and off-axis holography[10] based on different quasi-optical configurations. The greatest advantage of inline holographic imagers is the simple quasi-optical design. However, considerable efforts have to be made to suppress the effects of background and twin-image interferences in the reconstructed image. A feasible method to deal with this problem is to construct an off-axis reference wave to form a hologram with spatially separated terms and then to filter out the interferences, which is referred to as off-axis holography. Figure 1 shows a typical MMW off-axis holographic imager.[11] As shown in Fig. 1, a parabolic reflector is employed to realize the off-axis reference plane wave through collimating the radiation beam from the transmitting antenna, which interferes with the diffraction wave from the illuminated target. Then the interference pattern is recorded by the receiving antenna which scans over a certain aperture in the *xy* plane. The conventional MMW off-axis holographic imagers can effectively eliminate the interferences and reconstruct an image well. However, the limited illumination range on the target plane and limited reference wave aperture result in a relatively small field of view, which restricts the application of the MMW off-axis holography in imaging with large field of view. For instance, the synthesis of a reference plane wave with a large aperture brings great difficulty to the fabrication process. Moreover, the direction discrepancy of illuminated rays on a target plane may result in some image uniformity.

*Project supported by the National Natural Science Foundation of China (Grant Nos. 11174280, 60990323, and 60990320) and the Knowledge Innovation Program of the Chinese Academy of Sciences (Grant No. YYYJ-1123).

†Corresponding author. E-mail: xianggao1985@126.com
‡Corresponding author. E-mail: cli@mail.ie.ac.cn

© 2014 Chinese Physical Society and IOP Publishing Ltd

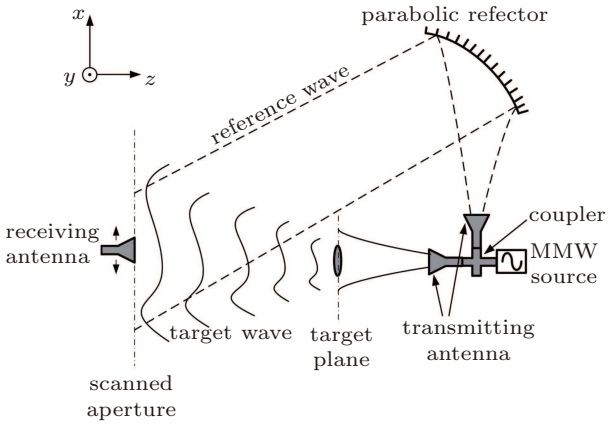


Fig. 1. Schematic diagram of a typical MMW off-axis holographic imager.

In this paper, an MMW squint indirect holographic scheme is presented which has a potential application in imaging with large field of view, such as short-distance personal screening in security check points. Instead of making efforts to design complex quasi-optics to realize an off-axis reference plane wave, the proposed system adopts the squint operation mode to enable the separation of interference terms, which achieves a similar effect to the off-axis holography but leaves out the large-aperture quasi-optical component. Besides this, the translational scanning of the quasi-optical platform contributes to a theoretically infinite field of view for the system and effectively ensures the image uniformity, which is difficult to implement in the conventional off-axis holographic imaging systems. In addition, the image reconstruction algorithm is studied for the proposed MMW imaging scheme. In the end, some imaging results on typical objects are obtained based on electromagnetic simulation, which demonstrates the good performance of the imaging scheme and its potential application in imaging with large field of view.

2. System description and image reconstruction algorithm

2.1. Imaging scheme description

Figure 2 shows the schematic plot of the MMW squint indirect holographic imager. The continuous wave signal generated from a monochromatic MMW source is transmitted by an MMW antenna. Then, the transmitting beam is equably separated into two parts with a semi-permeable beam splitter, one of which is reflected by a metal plate on the quasi-optical platform and the other scattered by a target with an oblique incident angle of θ. Based on the approach of division of amplitude, the two echoed waves (referred to as reference wave and target wave) come from the same wavefront of transmitting wave, which results in good spatial coherence between them. They interfere with each other, and form an interference pattern on the aperture of receiving antenna, of which the intensity is received and then detected by the MMW receiver. Data collection is performed by scanning the total quasi-optical platform over the xy plane with a scanning controller, the distance between the phase center of transmitting antenna and the imaging plane is kept to be d_1. Finally, the recorded data are sent to a computer for data processing and image reconstruction with a corresponding imaging algorithm.

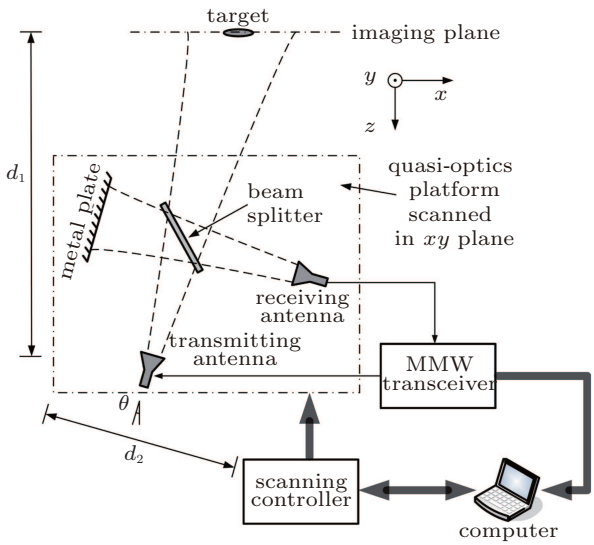


Fig. 2. Schematic diagram of the MMW squint indirect holographic imager.

Because of the fixed relative positions of the metal plate and the antennas during scanning, an invariable reference field is received which can be equivalent to a normal incident plane wave. On the other hand, the squint operation mode of the imager involves a nonzero Doppler central frequency for the target wave, which helps to spatially separate the interference terms within the hologram. Hence, a desired effect similar to the off-axis holography is achieved. In addition, the imager employs the translational scanning of the total quasi-optical platform to enlarge its field of view and ensure the image uniformity, which is different from the conventional off-axis holographic imaging systems. In these systems, the transmitting antenna is often immobile, which results in an unaltered interference diffraction wavefront then measured by a scanning receiving antenna. Hence, large field of view and image uniformity for these systems are very difficult to realize unless the illumination beam toward target plane and the reference beam toward receiving plane are both uniform plane waves within a large aperture.

2.2. Image reconstruction algorithm

In this section the details of an efficient algorithm are presented which is used to perform the image reconstruction for the MMW squint indirect holographic imager. To start with, the target to be imaged is assumed to be flat and characterized

by a reflectivity function $f(x,y)$ which is equal to the ratio of reflected field to incident field.

The total field E_t received by the receiving antenna can be denoted as the superposition of reference wave E_r and target wave E_s

$$\begin{aligned} & E_t\left(x',y'\right) \\ = & E_r\left(x',y'\right)+E_s\left(x',y'\right) \\ = & E_{r0}+\iint_s f\left(x,y\right)a\left(x-x',y-y'\right) \\ & \times \exp\left\{-j2k\left[\sqrt{(x-x')^2+(y-y')^2+d_1^2}\right]\right\}ds, \end{aligned} \quad (1)$$

where E_{r0} is a complex constant, k is the wave number in the free space, and $a(x-x',y-y')$ is a slowly varying amplitude factor which depends on the directivity of transmitting and receiving antenna.

Due to the squint operation mode, there exists an offset of $d_1\tan(\theta)$ between the coordinate x and x'. To unify the coordinate system, a translation transform is performed on the coordinate (x',y')

$$x'=x''-d_1\tan(\theta),\quad y'=y''. \quad (2)$$

Substituting Eq. (2) into Eq. (1), E_t can be further expressed as

$$\begin{aligned} & E_t(x''-d_1\tan(\theta),y'') \\ = & E_{r0}+\iint_s f(x,y)a(x-x''+d_1\tan(\theta),y-y'') \\ & \times\exp\left\{-j2k\left\{\sqrt{[x-x''+d_1\tan(\theta)]^2+(y-y'')^2+d_1^2}\right\}\right\}ds \\ = & E_{r0}+f(x'',y'')\otimes g(x'',y''). \end{aligned} \quad (3)$$

For convenience of writing, (x'',y'') is replaced to be (x,y), thus

$$E_t\left(x-d_1\tan\left(\theta\right),y\right)=E_{r0}+f\left(x,y\right)\otimes g\left(x,y\right), \quad (4)$$

where $g(x,y)$ is a point spread function and it can be denoted as

$$\begin{aligned} & g\left(x,y\right) \\ = & a\left(-x+d_1\tan\left(\theta\right),-y\right) \\ & \times\exp\left\{-j2k\left\{\sqrt{\left[x-d_1\tan\left(\theta\right)\right]^2+y^2+d_1^2}\right\}\right\}. \end{aligned} \quad (5)$$

The two-dimensional (2D) Fourier transform of $g(x,y)$ is the system function $G(\xi,\eta)$, which can be derived through the stationary phase method[12] as

$$\begin{aligned} & G\left(\xi,\eta\right) \\ = & a\left(\frac{\pi d_1\xi}{\sqrt{k^2-\pi^2\xi^2-\pi^2\eta^2}},\frac{\pi d_1\eta}{\sqrt{k^2-\pi^2\xi^2-\pi^2\eta^2}}\right) \\ & \times\exp\left[-j2d_1\sqrt{k^2-\pi^2\xi^2-\pi^2\eta^2}-j2\pi\xi d_1\tan\left(\theta\right)\right]. \end{aligned} \quad (6)$$

Reconsidering the physical meaning of the amplitude factor $a(x-x',y-y')$, it is found that $a(x-x',y-y')$ has a curve shape similar to a sinc^2 function and arrives at its maximum value where

$$x-x'=d_1\tan\left(\theta\right),\quad y-y'=0. \quad (7)$$

Hence, the central position (ξ_c,η_c) of system function $G(\xi,\eta)$ can be determined through solving Eq. (8) as

$$\begin{aligned} & \frac{\pi d_1\xi}{\sqrt{k^2-\pi^2\xi^2-\pi^2\eta^2}}=d_1\tan\left(\theta\right), \\ & \frac{\pi d_1\eta}{\sqrt{k^2-\pi^2\xi^2-\pi^2\eta^2}}=0, \end{aligned} \quad (8)$$

$$\begin{aligned} & \xi_c=\frac{k\sin\left(\theta\right)}{\pi}, \\ & \eta_c=0. \end{aligned} \quad (9)$$

For the MMW squint indirect holographic imager, only the amplitude of the echoed signal is measured by the MMW receiver. Hence, the output p of the receiver is directly proportional to $|E_t|^2$, which can be denoted as

$$\begin{aligned} & p\left(x,y\right) \\ = & \alpha\left|E_t\right|^2 \\ = & \alpha\left|E_{r0}+f\left(x,y\right)\otimes g\left(x,y\right)\right|^2 \\ = & \alpha\left|E_{r0}\right|^2+\alpha E_{r0}^*f\left(x,y\right)\otimes g\left(x,y\right) \\ & +\alpha E_{r0}f^*\left(x,y\right)\otimes g^*\left(x,y\right)+\alpha\left|f\left(x,y\right)\otimes g\left(x,y\right)\right|^2, \end{aligned} \quad (10)$$

where α is a positive real constant.

Applying the 2D Fourier transform to both sides of Eq. (10) yields

$$\begin{aligned} P\left(\xi,\eta\right) = & \alpha\left|E_{r0}\right|^2\delta\left(\xi,\eta\right)+\alpha E_{r0}^*F\left(\xi,\eta\right)G\left(\xi,\eta\right) \\ & +\alpha E_{r0}F^*\left(-\xi,-\eta\right)G^*\left(-\xi,-\eta\right) \\ & +\alpha\left[F\left(\xi,\eta\right)G\left(\xi,\eta\right)\right] \\ & \otimes\left[F^*\left(-\xi,-\eta\right)G^*\left(-\xi,-\eta\right)\right], \end{aligned} \quad (11)$$

where $F(\xi,\eta)$ is the Fourier transform of the reflectivity function $f(x,y)$ and may contain infinite spectrum components.

Figure 3 shows the spectrum distribution function $P(\xi,\eta)$ on the ξ axis. To separate the available term (second term) from other interference terms in Eq. (11), the central position ξ_c of system function $G(\xi,\eta)$ is at least 1.5 times as large as its critical bandwidth $\Delta\xi_{cr}$ on the ξ axis, i.e.,

$$\xi_c=\frac{k\sin\left(\theta\right)}{\pi}\geq 1.5\Delta\xi_{cr}. \quad (12)$$

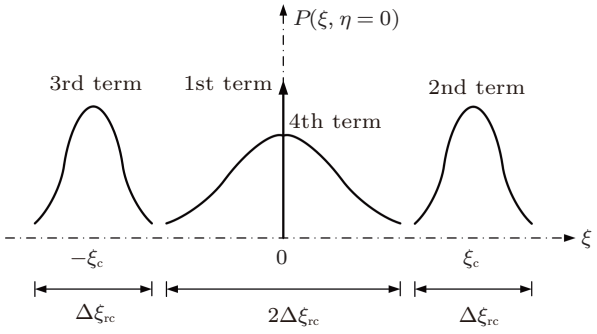


Fig. 3. Spectrum distribution function $P(\xi,\eta)$.

In fact, if the received scattered field from the target is far less than the reference field, the last term in Eq. (11) would be relatively small in comparison with the other three terms, and consequently it may be ignored. In that special case, equation (12) may be modified into

$$\xi_c = \frac{k\sin(\theta)}{\pi} \geq 0.5\Delta\xi_{cr}. \tag{13}$$

Compared with Eq. (13), equation (12) is a more strict one that is suitable for general situations, which hence requires a smaller sampling interval in the x direction to avoid the azimuth aliasing, i.e.,

$$d_x = \frac{1}{2(\xi_c + 0.5\Delta\xi_{cr})} \leq \frac{1}{4\Delta\xi_{cr}}, \tag{14a}$$

$$d_y \leq \frac{1}{2\Delta\eta_{cr}}, \tag{14b}$$

where d_x (d_y) is the sampling interval in the x (y) direction and $\Delta\eta_{cr}$ is the critical bandwidth of $G(\xi,\eta)$ on the η axis.

In the condition of the establishment of Eq. (12), a digital filtering operation with an appropriate window helps to extract the available second term of $P(\xi,\eta)$ and to remove other interference components. That is,

$$P_{lb}(\xi,\eta) = \alpha E_{r0}^* F(\xi,\eta) G(\xi,\eta). \tag{15}$$

To reconstruct the image of the target, a matched filtering function is defined as

$$H_{mf}(\xi,\eta) = \exp\left[\mathrm{j}2d_1\sqrt{k^2-\pi^2\xi^2-\pi^2\eta^2} + \mathrm{j}2\pi\xi d_1\tan(\theta)\right]. \tag{16}$$

Finally, a focused image characterized by $\tilde{f}(x,y)$ is obtained through multiplying $P_{lb}(\xi,\eta)$ with $H_{mf}(\xi,\eta)$ and then performing an inversed fast Fourier transform (IFFT) on the product, i.e.,

$$\begin{aligned}\tilde{f}(x,y) &= \mathrm{IFFT}[P_{lb}(\zeta,\eta)H_{mf}(\zeta,\eta)] \\ &= \mathrm{IFFT}[\alpha E_{r0}^* F(\zeta,\eta)A(\zeta,\eta)] \\ &= \alpha E_{r0}^* f(x,y) \otimes \mathrm{IFFT}[A(\zeta,\eta)],\end{aligned} \tag{17}$$

where $A(\xi,\eta)$ is a weight factor whose 6-dB (roundtrip) bandwidth ($\Delta\xi_{6\ \mathrm{dB}}$, $\Delta\eta_{6\ \mathrm{dB}}$) determines the final spatial resolution of the image and it can be denoted as

$$A(\xi,\eta) = a\left(\frac{\pi d_1\xi}{\sqrt{k^2-\pi^2\xi^2-\pi^2\eta^2}}, \frac{\pi d_1\eta}{\sqrt{k^2-\pi^2\xi^2-\pi^2\eta^2}}\right). \tag{18}$$

As seen from Eq. (18), the 6-dB bandwidth of $A(\xi,\eta)$ is indeed determined by the directivity of the antenna, more exactly the half-power beam widths (HPBWs) $\theta_{x_3\ \mathrm{dB}}$ and $\theta_{y_3\ \mathrm{dB}}$. Considering the geometrical relations shown in Fig. 2, the beam width on the imaging plane is derived as

$$\Delta x_{3\ \mathrm{dB}} = \frac{2d_1}{\cos^2(\theta)}\tan(\theta_{x_3\ \mathrm{dB}}/2), \tag{19a}$$

$$\Delta y_{3\ \mathrm{dB}} = \frac{2d_1}{\cos(\theta)}\tan(\theta_{y_3\ \mathrm{dB}}/2), \tag{19b}$$

where θ is the squint angle. On the other hand, based on Eq. (18), $\Delta x_{3\ \mathrm{dB}}$ and $\Delta y_{3\ \mathrm{dB}}$ can also be expressed, respectively, as

$$\begin{aligned}\Delta x_{3\ \mathrm{dB}} &= \frac{\partial}{\partial\xi}\left(\frac{\pi d_1\xi}{\sqrt{k^2-\pi^2\xi^2-\pi^2\eta^2}}\right)\Bigg|_{\xi_c,\eta_c}\Delta\xi_{6\ \mathrm{dB}} \\ &= \frac{\pi d_1}{k\cos^3(\theta)}\Delta\xi_{6\ \mathrm{dB}},\end{aligned} \tag{20a}$$

$$\begin{aligned}\Delta y_{3\ \mathrm{dB}} &= \frac{\partial}{\partial\eta}\left(\frac{\pi d_1\eta}{\sqrt{k^2-\pi^2\xi^2-\pi^2\eta^2}}\right)\Bigg|_{\xi_c,\eta_c}\Delta\eta_{6\ \mathrm{dB}} \\ &= \frac{\pi d_1}{k\cos(\theta)}\Delta\eta_{6\ \mathrm{dB}}.\end{aligned} \tag{20b}$$

Then, the 6-dB bandwidth ($\Delta\xi_{6\ \mathrm{dB}}$, $\Delta\eta_{6\ \mathrm{dB}}$) of $A(\xi,\eta)$ can be derived through combining Eq. (19) with Eq. (20) as

$$\Delta\xi_{6\ \mathrm{dB}} = \frac{2k}{\pi}\tan(\theta_{x_3\ \mathrm{dB}}/2)\cos(\theta), \tag{21a}$$

$$\Delta\eta_{6\ \mathrm{dB}} = \frac{2k}{\pi}\tan(\theta_{y_3\ \mathrm{dB}}/2). \tag{21b}$$

According to Eq. (17), the spatial resolution of the MMW squint indirect holographic imager is approximately 0.886 times the reciprocal of the 6-dB bandwidth of $A(\xi,\eta)$, as shown below

$$\delta_x = \frac{0.886}{\Delta\xi_{6\ \mathrm{dB}}} = \frac{0.443\pi}{k\cos(\theta)\tan(\theta_{x_3\ \mathrm{dB}}/2)}, \tag{22a}$$

$$\delta_y = \frac{0.886}{\Delta\eta_{6\ \mathrm{dB}}} = \frac{0.443\pi}{k\tan(\theta_{y_3\mathrm{dB}}/2)}. \tag{22b}$$

3. System design and simulation

To demonstrate the performance of the MMW squint indirect holographic imaging scheme, a 0.2-THz prototype system is designed based on some equations given above and simulated with some efficient electromagnetic analysis methods.

The final imaging distance d_1 is chosen to be 0.3 m and the metal plate on the platform is about 0.1 m away from the receiving antenna aperture. The transmitting and receiving antennas are two identical dual-mode conical horns polarized in

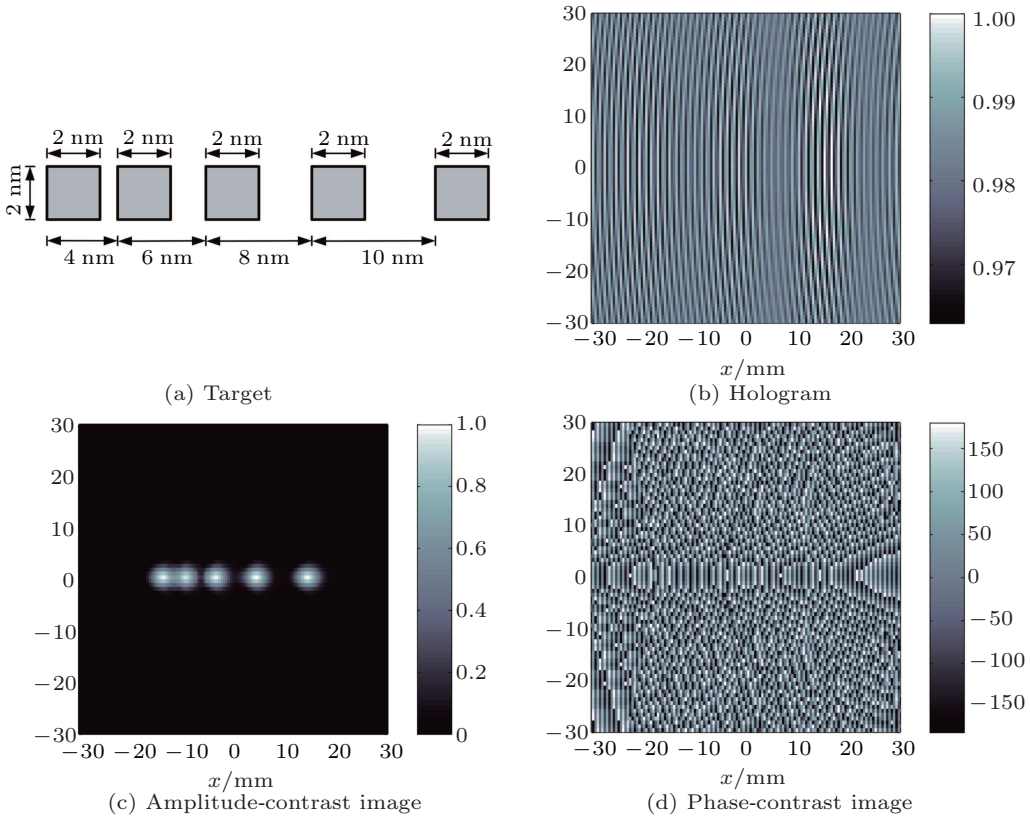


Fig. 4. (color online) Simulation results of five small metal targets arranged in the *x* direction.

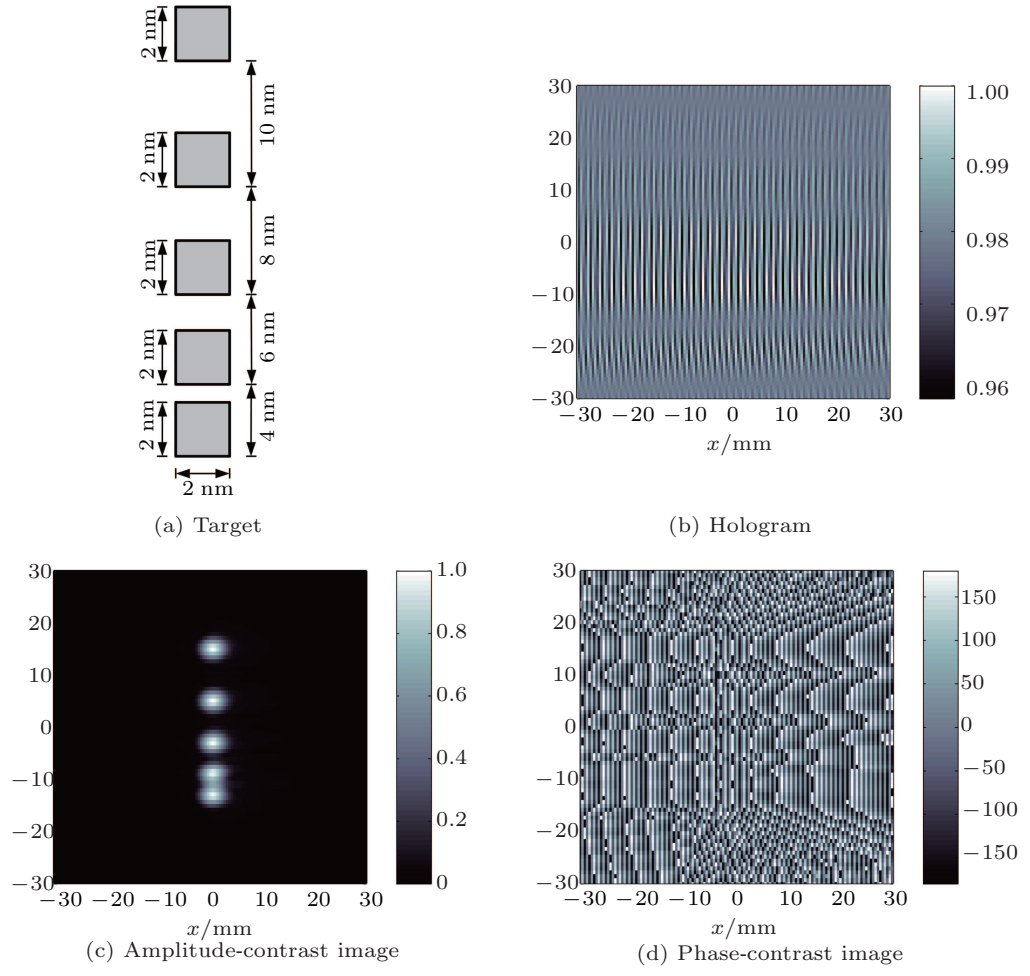


Fig. 5. (color online) Simulation results of five small metal targets arranged in the *y* direction.

the y direction. Optimized by the multilevel fast multipole algorithm (MLFMA), each horn has a circular aperture with a diameter of 7.5 mm and a symmetrical pattern with an HPBW of 16°. In the condition of a squint angle of 38°, the spatial resolutions in x and y directions can be calculated based on Eq. (22) to be 3 mm and 2.4 mm respectively. To sufficiently remove the interference terms in $P(\xi,\eta)$, the critical bandwidth $\Delta\xi_{\rm cr}$ is set to be 1.8 times the $\Delta\xi_{6\ {\rm dB}}$, which means that the boundary level achieves about -20 dB relative to the peak value. For these design parameters, equation (12) is obviously satisfied. Besides this, according to Eq. (14), the sampling interval is 0.45 mm in the x direction, and it is 0.75 mm in the y direction.

Based on the combination of reciprocity theorem and physical optics (PO) method, an electromagnetic simulation is performed with the designed prototype system. Figure 4 shows the simulated results of five 2 mm $\times$ 2 mm metal targets arranged in the x direction, with spaces of 2 mm, 4 mm, 6 mm, and 8 mm. Figures 4(b)–4(d) are the hologram, reconstructed amplitude-contrast image, and phase-contrast image, respectively, of the targets shown in Fig. 4(a). As shown in Fig. 4(c), the square targets are well distinguished except for the first and second one because of the 3-mm resolution in the x direction, which validates the effectiveness of MMW squint indirect holographic algorithm. Due to the non-zero central frequency of $A(\xi,\eta)$, there exists an accessional phase factor in the reconstructed phase-contrast image (Fig. 4(d)). Figure 5 shows that the imaging results of the targets are the same as those in Fig. 4(a) but arranged in the y direction, which also demonstrates the good performance of the proposed imaging scheme and image reconstruction algorithm.

4. Conclusion

An MMW squint indirect holographic imaging scheme is presented in this paper. Based on the squint operation mode, the proposed system employs simple quasi-optics to achieve a similar effect to off-axis holography. Moreover, the translational scanning of the total quasi-optical platform helps to produce a large field of view and ensure the image uniformity, which is difficult to realize in the conventional off-axis holography. Imaging results on typical targets demonstrate the effectiveness of the imaging scheme and its potential applications in MMW imaging with a large field of view.

References

[1] Gabor D 1948 *Nature* **161** 777

[2] Zhang Q S, Lü X X, Yu Q T and Liu G Y 2009 *Chin. Phys. B* **18** 2764

[3] Tamminen A, Laurinaho J A and Raisanen A V 2008 *European Radar Conference*, October 30–31, 2008, Amsterdam, Netherlands, p. 168

[4] Heimbeck M S, Kim M K, Gregory D A and Everitt H O 2011 *Opt. Express* **19** 9192

[5] Adametz J, Gumbmann F and Schmidt L P 2011 *6th German Microwave Conference*, March 14–16, 2011, Darmstadt, Germany, p. 1

[6] Sheen D M, McMakin D L, Hall T E and Severtsen R H 2009 *IEEE Conference on Technologies for Homeland Security*, May 11–12, 2009, Waltham, USA, p. 440

[7] Appleby R and Wallace H B 2007 *IEEE Trans. Antennas Propag.* **55** 2944

[8] Gao X, Li C, Gu S M and Fang G Y 2012 *IEEE Antennas and Wireless Propaga. Lett.* **11** 787

[9] Xue K, Li Q, Li Y D and Wang Q 2012 *Opt. Lett.* **37** 3228

[10] Leach M, Elsdon M, Foti S J and Smith D 2006 *Microwave Opt. Technol. Lett.* **48** 1957

[11] Mahon R J, Murphy J A and Lanigan W 2006 *Opt. Commun.* **260** 469

[12] Carrier G F, krook M and Pearson C E 1966 *Functions of a Complex Variable* (New York: McGraw-Hill), p. 257